PAUL SCHERRER INSTITUT

PSI Bericht Nr. 96-20
November 1996
ISSN 1019-0643

Projekt Synchrotronlichtquelle

A New Treatment of Focusing by Varied-line-spacing Gratings with Application to the Peterson PGM System

M. R. Howells, U. Staub

Paul Scherrer Institut
CH - 5232 Villigen PSI
Telefon 056 310 21 11
Telefax 056 310 21 99

A NEW TREATMENT OF FOCUSING BY VARIED-LINE-SPACING GRATINGS WITH APPLICATION TO THE PETERSEN PGM SYSTEM

M. R. Howells[1] and U. Staub[2]

[1]Advanced Light Source, Lawrence Berkeley National Laboratory, Berkeley, CA 94720, USA.

[2]Swiss Light Source, Paul Scherrer Institut, CH-5232 Villigen PSI, Switzerland.

October 15 1996

Abstract

We present a new treatment for a varied-line-spacing grating (VLS) as a monochromator for a soft X-ray synchrotron beamline. Our calculations for a VLS monochromator show that within the small angle approximation we can make the focal length constant, correct for primary coma and spherical aberrations at all wave lengths. This monochromator scheme has still a free choice of included angle, which can be used to optimize efficiency and it can cover a wave length range of eight octaves, distinct more compared to a plane grating monochromator scheme. The analytical calculations are in excellent agreement with our ray traces using the Shadow computer code.

Background

The use of varied-line-spacing (VLS) monochromator designs has been established in the synchrotron beam-line field for about a decade due to the work of Hettrick[1-4], Underwood[5], Harada[6-8], Koike[9-11], Namioka[12], Höscht[13], McKinney[14, 15], Palmer[16, 17] and Callcott[18] with various collaborators. However, the number of beam lines currently operating with this type of system is quite small (less than ten) and there is not yet a variable-included-angle device in operation although there are plans for at least one[10].

The original purpose of introducing VLS schemes was often said to be to avoid the sliding exit slits that were used on the standard (fixed-included-angle) spherical grating monochromators (SGM's). However, there are many schemes which avoid such sliding of the exit slit without using VLS and we believe that such a limited purpose does not do full justice to the power of the VLS principle. We discuss some of its other advantages below.

The SGM's were a good response to the challenges of their day but they have some definite limitations. These are (i) the requirement for moving the slits to preserve focus as the wavelength is scanned, (ii) the constant deviation angle which implies an inability to suppress high orders, (iii) the limited wavelength coverage (about one octave) per grating and consequent breaks in the wavelength scan, (iv) relatively poor tracking of the efficiency maximum on the efficiency-incidence-angle plot (efficiency map) especially in positive order and (v) the fact that suppression of the aberration known as "primary coma" in the synchrotron-radiation community [footnote] is normally achieved at only one wavelength; the Rowland wavelength. Some of these issues can be addressed using the Petersen plane-grating monochromator (PGM)[19] concept or later variations thereof. Such designs provide a much better wavelength coverage per grating, reasonable tracking of the maximum on the efficiency map and exact focus without slit motions. However, the included angle must be programmed to a particular value at each wavelength to achieve focus and so orders can still not be suppressed and the primary coma of the grating cannot be properly corrected.

There are two possible enhancements to the Petersen monochromator which can in principle avoid the need to program the included angle: an adaptive mirror and a VLS grating. We discuss only the latter in this report although we believe both are viable. The advantage of the VLS approach is that it provides a passive solution which only needs to be "built in" at the construction phase. The disadvantage is the difficulty of obtaining VLS gratings.

The most usual practice in VLS systems is to illuminate the grating with a converging beam. Thus the present-day VLS plane-grating schemes tend to look like a Petersen or Miyake system in reverse. However, there appears to be no reason why they should not be used in the normal direction i.e. with a *diverging* beam on the grating. In fact, by the principle of reversibility of light, the virtual image produced by the grating with a diverging beam should have all the same properties as the real image produced using a converging beam. Therefore, it should be possible to simply replace the grating in a standard SX700

system with a VLS optic. As explained below this would not only ensure that the system remained almost exactly in focus during wavelength scanning *without* programming the included angle but the focus would also become stigmatic. The principal complication of the plan would be that the best VLS performance is achieved with a grating magnification of -1 which is not the value used in the standard SX700 system. Therefore, one would also have to change the focal length of the mirror.

The basic principles of VLS

The advocates of VLS have not always explained the idea to the community in a clear way. This was in part because some authors regarded the matter as proprietary[20]. Notable exceptions were Callcott et al.[18], who gave an ab initio analysis, Palmer and McKinney[16] and McKinney[15]. The last-named reference provides derivations of the equations in the Hettrick-Underwood patent and also gives the basic design data for VLS systems, namely the terms of the optical path function.

In this report we use the McKinney terms to show that within the limits of the small-angle approximation the VLS plane grating has the following remarkable properties which apply for all values of the incidence and diffraction angles, in other words all wavelengths.

1. The focal length of the grating can be made constant.
2. The primary coma of the grating can be corrected.
3. That, if 1. and 2. are done, the spherical aberration of the grating is also automatically corrected.

Thus within the stated limit we have *universal solutions* for the correction of focus and the other important in-plane aberrations. The corrections are good over the wavelength range for which the sines of the grazing angles of incidence and diffraction can be approximated by the angles. We will show below that, in practice, they are sufficiently good over at least the normal working range of a Petersen PGM and in the example we take they are good over eight octaves without a change of grating.

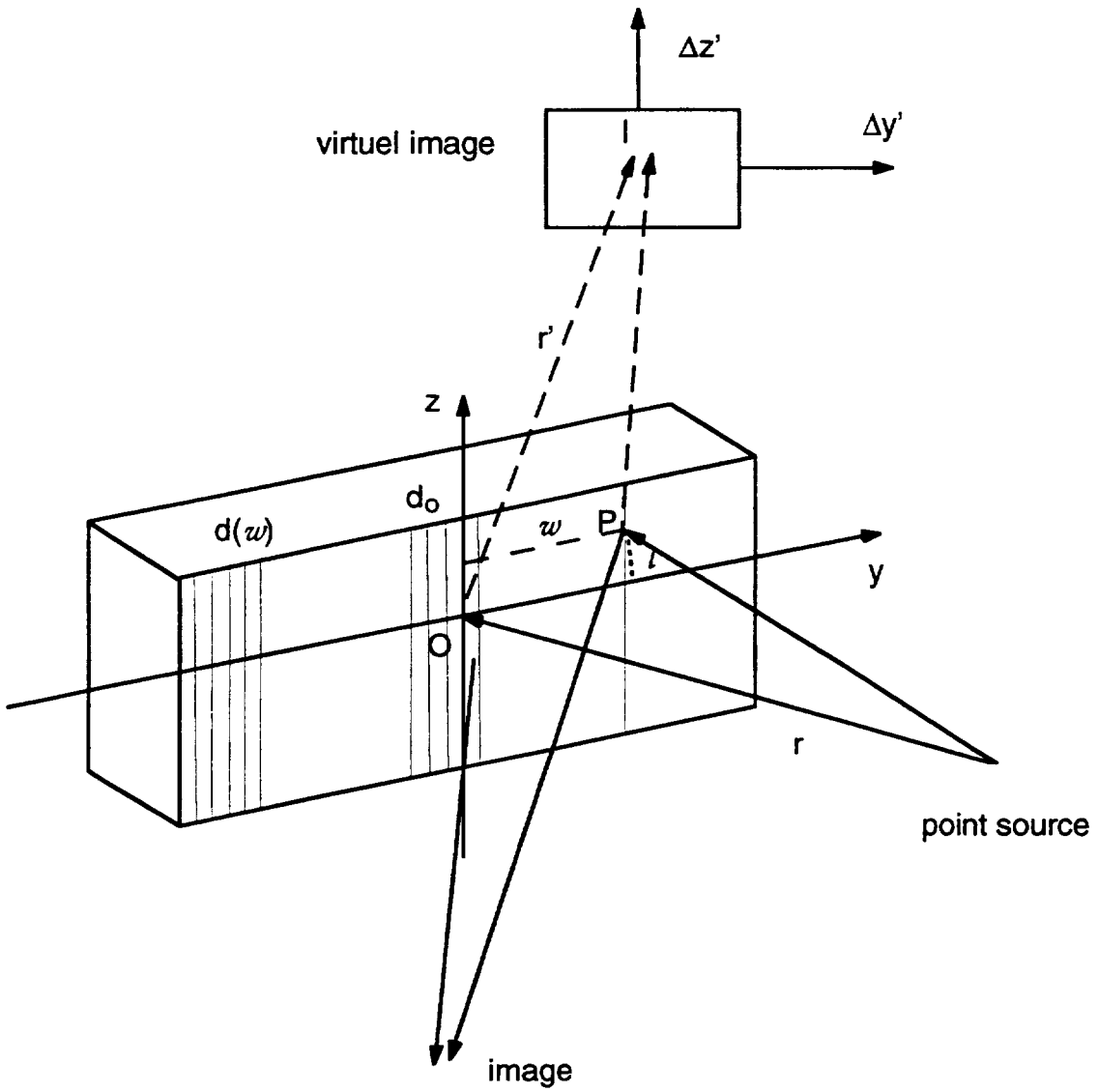

Fig 1. Schematic view of the grating monochromator

We consider the focal length first and define the groove spacing of the VLS grating to be given by

$$d(w) = d_0\left(1 + v_1 w + v_2 w^2 + \mathrm{K}\right), \tag{1}$$

where apart from the VLS coefficients v_i we are using the geometry and notation of Noda et al.[21]. This is shown in Fig. 1 where P is a general point (w, l) on the grating surface. In the general theory, the shape of the grating is described in terms of a MacLaurin series $x = \sum a_{ij} y^i z^j$. However, for the present purpose we consider only a plane grating (x=0) in

which case all the a_{ij}'s are zero. In general the 200 (focusing) term of the optical path function[15] is

$$(F)_{200} = \frac{1}{2}w^2\left\{T + T' - \frac{\nu_1 m\lambda}{d_0}\right\}$$
$$\text{where } T = \left(\frac{\cos^2\alpha}{r} - 2a_{20}\cos\alpha\right) \text{ and } T' = \left(\frac{\cos^2\beta}{r'} - 2a_{20}\cos\beta\right) \tag{2}$$

and the condition for focus is therefore $(F)_{200}=0$. Specializing to the plane grating by putting $a_{20}=0$, substituting for $m\lambda/d_0$ using the grating equation and switching to grazing angles $a = \pi/2 - |\alpha|,\ b = \pi/2 - |\beta|$, the condition for focus becomes

$$\frac{1}{r'} = \nu_1\frac{\cos a - \cos b}{\sin^2 b} - \frac{1}{r}\frac{\sin^2 a}{\sin^2 b} = \frac{1}{r}\left\{\nu_1 r\frac{-2\sin\left(\frac{a+b}{2}\right)\sin\left(\frac{a-b}{2}\right)}{\sin^2 b} - \frac{\sin^2 a}{\sin^2 b}\right\}. \tag{3}$$

Now approximating $\sin a \cong a$ etc. we arrive at

$$\frac{1}{r'} = \frac{1}{r}\left\{-\nu_1 r\frac{a^2 - b^2}{2b^2} - \frac{a^2}{b^2}\right\} \tag{4}$$

Evidently if $\nu_1 = \frac{-2}{r}$ then $r' = -r$ *identically* for all values of a and b. For illumination by a real point source, we then get a virtual image at a constant distance equal to the source distance. This means that within the limitations of the small-angle approximation, the system is both in focus and stigmatic for all wavelengths. For this choice of ν_1 the exact focal length is obtained by solving $(F)_{200}=0$ without the small-angle approximation as follows

$$r' = \frac{\cos^2\beta}{\nu_1(\sin\alpha + \sin\beta) - \frac{\cos^2\alpha}{r}} = \frac{-r\cos^2\beta}{2(\sin\alpha + \sin\beta) + \cos^2\alpha}. \tag{5}$$

Turning to the question of coma correction we have[15]

$$(F)_{300} = \frac{1}{2}w^3\left\{\frac{T\sin\alpha}{r} + \frac{T'\sin\beta}{r'} - 2a_{30}(\cos\alpha + \cos\beta) + \frac{2}{3}\left(\nu_1^2 - \nu_2\right)\frac{m\lambda}{d_0}\right\} \tag{6}$$

Following a similar procedure as before, we find that the condition that $(F)_{300}=0$ is

$$\frac{a^2}{r^2}-\frac{b^2}{r'^2}+\frac{2}{3}\left(v_1^2-v_2\right)\left(\frac{b^2-a^2}{2}\right)=0. \tag{7}$$

Now setting $v_1=\frac{-2}{r}$ and $r'=-r$ we find that if $v_2=\frac{1}{r^2}$, the coma vanishes identically for all values of a and b and thus for all wavelengths so long as a and b are small.

Applying similar arguments to the spherical aberration term[15]

$$(F)_{400}=\frac{1}{8}w^4\left\{\begin{array}{l}\dfrac{4T\sin^2\alpha}{r^2}+\dfrac{4T'\sin^2\beta}{r'^2}-\dfrac{T^2}{r}-\dfrac{T'^2}{r'}+4a_{20}^2\left(\dfrac{1}{r}+\dfrac{1}{r'}\right)-8a_{30}\left(\dfrac{\sin\alpha\cos\alpha}{r}+\dfrac{\sin\beta\cos\beta}{r'}\right)\\ -8a_{40}(\cos\alpha+\cos\beta)-2\left(v_1^3-2v_1v_2+v_3\right)\dfrac{m\lambda}{d_0}\end{array}\right\}$$

, (8)

we find that $(F)_{400}=0$ if

$$\frac{a^2}{r^3}\left(4-5a^2\right)+\frac{b^2}{r'^3}\left(4-5b^2\right)=\left(v_1^3-2v_1v_2+v_3\right)\left(b^2-a^2\right). \tag{9}$$

Substituting the conditions $v_1=\frac{-2}{r}$, $v_2=\frac{1}{r^2}$ and $r'=-r$ and neglecting terms of fourth order and above in a and b, we find that $(F)_{400}$ vanishes identically for all a and b if $v_3=0$. So that, if the focus and coma are corrected as proposed, then the correction of the spherical aberration follows automatically, again within the limitations of the small-angle approximation.

The aberration-correcting combination of parameters can thus be summarized as

$$v_1=\frac{-2}{r},\ v_2=\frac{1}{r^2}\ \text{and}\ r'=-r \tag{10}$$

The simplicity of these solutions strongly suggests that the description of the VLS grating in terms of a power series in the groove spacing, rather than the density, is more naturally related to the normally recognized optical aberrations.

Comparison of the predicted performance of the plane grating with the SHADOW ray trace code

We have carried out ray traces to check the statements made in the previous section. They are of the *plane grating alone* using the SHADOW code with a point source. This means that the obtained spot patterns (shown in Figs. 2-5) are those of the virtual image of the source. The parameters used were as follows:

Quantity	Unit	Value
Center groove spacing (d_0)	Å	16666.667 (600/mm)
Incidence angle (α)	degree	86
v_1	m^{-1}	-0.1333333
v_2	m^{-2}	0.0044444 or 0.0000
Order (m)		+1 (inside)*
Illuminated half width (w_{max})	mm	17.8
Change in groove spacing: w=0 to w_{max}	%	0.22
Wavelength (λ)	Å	40
Source-to-grating distance (r)	m	15.00
Grating-to-receiving-plane distance (r')	m	-15.00 or -14.9729**
Source half angle (tangential plane)	milliradian	0.083
Source half angle (sagittal. plane)	milliradian	1.00
Beam full widths at grating: tan.×sag.	mm^2	25×30
Numbers of rays : tan.×sag.		21×5

*For SHADOW the convention is to use -1 for inside order.

**-15 m is the small-angle result for the focal distance and -14.9729 m is the exact one from eq. (5)

The grating VLS coefficients that we have used have to be translated into the SHADOW notation which is based on the groove density s=1/d so that we have

$$s(w) = s_0 + s_1 w + s_2 w^2 + \mathrm{K}$$
$$= s_0\left(1 + \frac{s_1}{s_0} w + \frac{s_2}{s_0} w^2 + \mathrm{K}\right) \equiv \frac{1}{d_0\left(1 + v_1 w + v_2 w^2 + \mathrm{K}\right)}$$

By considering the case $w \to 0$ we see that $s_0 = \frac{1}{d_0}$ and the formula for the reciprocal of a series in the above form is given, can easily be received by a Taylor expansion. This gives the

following translations for the cases of focus correction only (left side) and focus and coma correction (right side).

VLS GROOVE DEFINITIONS		
(Focus corrected)		
Source dist (m)=	15	
Center gr/mm=	600	
d0=	0.000166667	cm
v1=	-0.001333333	cm^-1
v2=	0	cm^-2
v3=	0	cm^-3
v4=	0	cm^-4
s0=	6000	cm^-1
s1=	8	cm^-1
s2=	0.010666667	cm^-2
s3=	1.42222E-05	cm^-3
s4=	1.8963E-08	cm^-4

VLS GROOVE DEFINITIONS		
(Focus and coma corrected)		
Source dist (m)=	15	
Center gr/mm=	600	
d0=	0.000166667	cm
v1=	-0.001333333	cm^-1
v2=	4.44444E-07	cm^-2
v3=	0	cm^-3
v4=	0	cm^-4
s0=	6000	cm^-1
s1=	8	cm^-1
s2=	0.008	cm^-2
s3=	7.11111E-06	cm^-3
s4=	5.92593E-09	cm^-4

By calculating the groove density exactly (s=1/d) and by the fourth order approximation we can conclude that in the present case the approximation is correct to twelve significant figures which is sufficient.

It is noteworthy that one can obtain correction of the focus by a proper choice of either v_1 with the higher v's equal to zero or s_1 with the higher s's equal to zero. However, these solutions are not equivalent and they have different amounts of coma and higher order aberrations. One can see this for example by noting that the Taylor series of $\frac{1}{1+v_1 w}$ has an infinite number of non zero terms. It is also evident from the ray traces.

First consider the tangential aberrations (vertical on the spot diagram) of the ray trace of the VLS grating with focus-only correction (Fig. 2). This ray trace is taken at the exact focus position determined by equation (5). To within a good approximation each group of 21 spots are in pairs with each spot on top of its partner. This is true within less than 0.03 μm. Evidently the pairs arise because the rays at $\pm w$ are aberrated in the same direction and by the same amount indicating that the lowest order ray aberration varies like w^2 and that defocus (which varies like w) is absent. This shows that our calculation of the focal distance is correct. That the w^2 aberration is in fact the dominant one in the tangential plane is confirmed by noting that, to a good approximation, the deflection of the rays at $\pm w_{max}$ is *four* times greater than those at $\pm w_{max}/2$. We can also calculate the amount of deflection by theory (see, for example, The X-ray Data Booklet[23] for a prescription for calculating specific ray aberrations $\Delta y'_{ij}$ and $\Delta z'_{ij}$ from the corresponding terms of F. For the coma term we have

$$\Delta y'_{300} = \frac{r'}{\cos\beta}\frac{\partial}{\partial w}(F)_{300} \tag{11}$$

where $(F)_{300}$ is given by (6). For the rays at $\pm w_{max}$ this gives the value 0.529 μm (Δ_{coma} in Appendix 1) for the present case which agrees well with the ray trace.

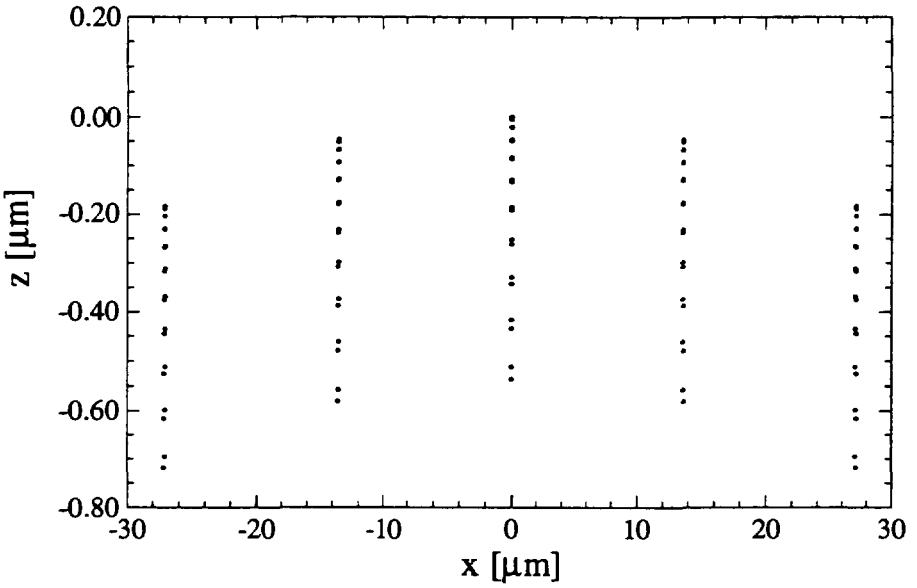

Fig. 2. Ray trace calculation using the Shadow code for the virtual image of a VLS with focal length correction using a point source. (at focal length)

In the sagittal direction the five groups of rays are spaced uniformly either side of center indicating that the dominant aberration is astigmatism. The amount of astigmatism is equal to

$$\Delta z'_{020} = r'\frac{\partial}{\partial z}(F)_{020} = r'l(S+S') = l\frac{\Delta r}{r}$$
$$\text{where } S = \frac{1}{r} - 2a_{02}\cos\alpha, \qquad S' = \frac{1}{r'} - 2a_{02}\cos\beta \tag{12}$$

and Δr is the distance between the tangential and sagittal foci. Thus for the present case, Δr=27.1 mm (focal length in Appendix 1) and we get $(\Delta z'_{020})_{max} = 27$ μm in good agreement with the ray trace.

The other aberration that can be seen in Fig 2 is the quadratic curvature of the focal line which is not an aberration of the form $F_{ijk} \approx F_{i00}$ and so is not determined by the VLS properties of the grating. Allowing for the fact that $\Delta z' \propto l$ because astigmatism is normally

the dominant sagittal aberration, we can see that such quadratic curvature $\left(\Delta y' \propto \Delta z'^2\right)$ can be produced by the 120, 111 and 102 terms of the optical path function[24, 25]. Thus for an in-plane point source ($z = 0,\ z' = \Delta z'$), the line-curvature (lc) terms are

$$(F)_{lc} = \frac{1}{2} w l^2 F_{120} + \frac{1}{2} w F_{102} + w l F_{111} = \frac{1}{2} w l^2 \left\{ \frac{S \sin\alpha}{r} + \frac{S' \sin\beta}{r'} \right\} + \frac{1}{2} w \frac{\Delta z'^2 \sin\beta}{r'^2} - w l \frac{\Delta z' \sin\beta}{r'^2}$$

. (13)

Substituting from eq. (12) for l and specializing to the case of a plane grating this gives

$$\left(\Delta y'_{lc}\right)_{\max} = \frac{r'}{\cos\beta} \frac{\partial}{\partial w} (F)_{lc} = \frac{l^2_{\max}}{2} \frac{r'}{\cos\beta} \left\{ \frac{\sin\alpha + \sin\beta}{r^2} \right\} \tag{14}$$

Evaluating this for the case at hand ($\Delta y'_{lc}$ in Appendix 1) we get 0.183 μm in very good agreement with the ray trace.

Continuing to study the ray distribution at the exact focus we now consider what happens when we have both focus and coma correction in place. That is both v_1 and v_2 have the values given by eq. 10. The ray trace (Fig. 3) is the same as before except the 0.529 μm spread of rays in the vertical direction which we attributed to coma has now been compressed down to about 0.01 μm showing that the coma has been correctly canceled as intended. The quadratic line curvature and small higher order aberrations remain in place.

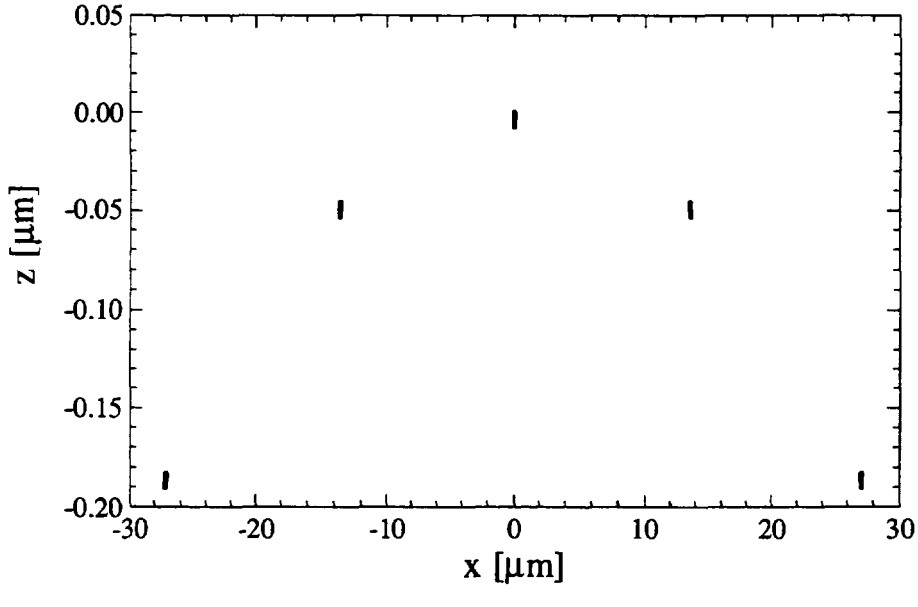

Fig. 3. Ray trace calculation using the Shadow code for the virtual image of a VLS with focal length and coma correction using a point source. (at focal length)

We now turn to the ray patterns received around the axial point (I in Fig. 1) at the exact source distance behind the grating (r'=-r). This point is the position of the sagittal focus for all wavelengths. With v_1 equal to -2/r and v_2=0 we get the distribution shown in Fig. 4. We see that the overall sagittal width of the pattern $2\Delta z'_{max}$ has dropped from 54 μm to 0.08 μm and when w=0, the width $\Delta z'$=0 for all l. Both of these features are due to the vanishing of the astigmatism. When l=0 (in-plane rays) the dominant aberration is defocus. The other significant aberrations are coma (displacements proportional to w^2) and line curvature. However, since the astigmatism is now zero we cannot make the substitution from eq. (12) for l in eq. (13). Rather we must set $\Delta z'$=0 in eq. (13) which eliminates the 102 and 111 terms leaving only the 120 term. With r'=-r this leads to an unchanged expression for the line curvature $\Delta y'_{lc}$ (eq. (14)) and

$$(\Delta z')_{120} = wl\frac{r'}{\cos\beta}\left\{\frac{\sin\alpha+\sin\beta}{r^2}\right\} \tag{15}$$

We can now see which aberrations are at work in Fig. 4. The dominant tangential one is defocus ($\Delta y'$ varying linearly with w). The dominant sagittal one is astigmatic coma ($\Delta z'$

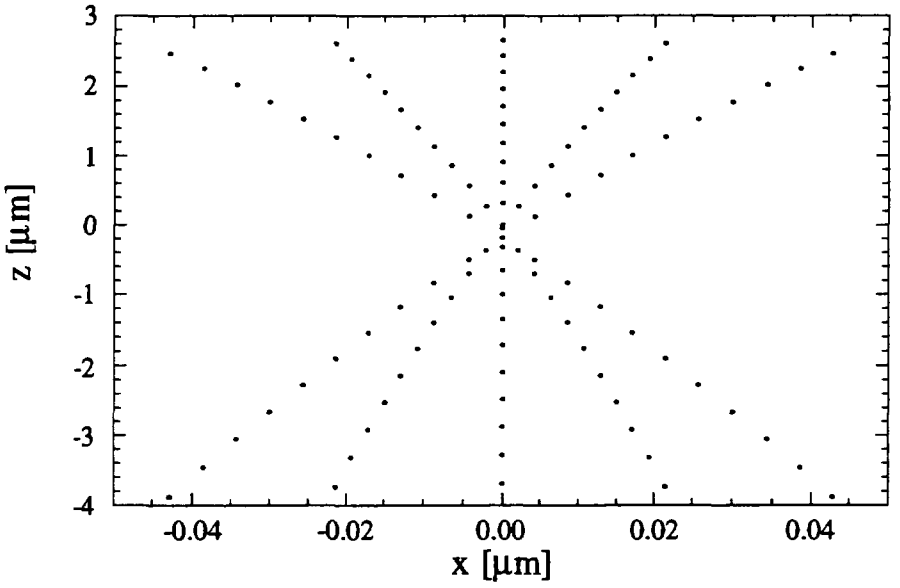

Fig. 4. Ray trace calculation using the Shadow code for the virtual image of a VLS with focal length correction using a point source. (at r=-r')

varying linearly with w for a given l value (eq. (15)). The results are the five crossed lines with equally-spaced spots that are seen in Fig. 4. Each corresponds to a constant l value and has a slope proportional to l . The two more subtle aberrations which are nonetheless visible are coma and line curvature. The former adds a displacement proportional to w^2 which is a quadratic curvature for each line l=constant. The latter, which is the same quadratic curvature we had before, adds a displacement proportional to $\Delta z'^2$ (and therefore to l^2) to each line w=constant.

Finally, the pattern shown in Fig. 5 is the same as Fig. 4 except that coma correction has been included. One can see that the curvature of the lines l=constant has now disappeared as intended, again confirming the validity of the coma-correcting procedure described earlier.

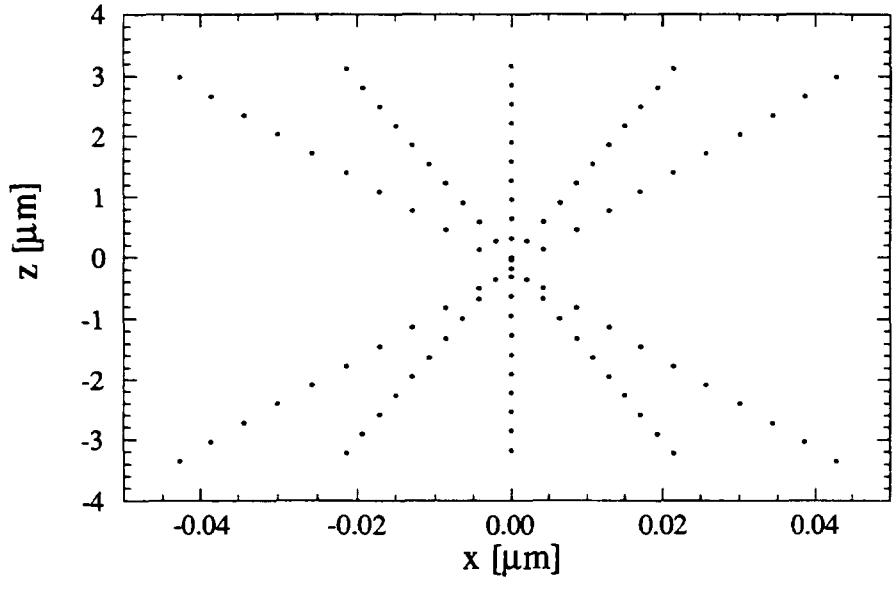

Fig. 5. Ray trace calculation using the Shadow code for the virtual image of a VLS with focal length and coma correction using a point source. (at r=-r')

Some performance parameters for a real Petersen PGM system

We are trying to understand how useful the VLS concept is in the context of what seems now to be the "standard" Petersen-system configuration incorporating the original rotating plane mirror, a plane grating and a spherical focusing mirror. To pursue this question we first consider the simplest possible system of this class with only one grating and no entrance slit. The incoming beam is considered to be roughly like an undulator beam from a third-generation synchrotron light source. The source is taken to be of size 0.1 mm and distance 15 m delivering a beam of height 2.5 mm. We make no attempt to model a realistic undulator

source, indeed the theoretical range of the monochromator, 5-1280 Å, which is eight octaves, is much greater than most undulators can cover. The most important point to note is that this design has a *free choice of included angle.* The incidence angles (α) used in the spread sheet were chosen to give a very rough optimization of the scalar-theory efficiency but they could be anything within the mechanical and reflectance limits. Once α is chosen the diffraction angle follows from the grating equation.

We calculate in the spread sheets of Appendix 1, the contributions of the important aberrations to the broadening of the virtual image and the consequent effects on the resolution. We also estimate various other contributions to the resolution and make a scalar-theory calculation of the grating efficiency (Fig. 6).

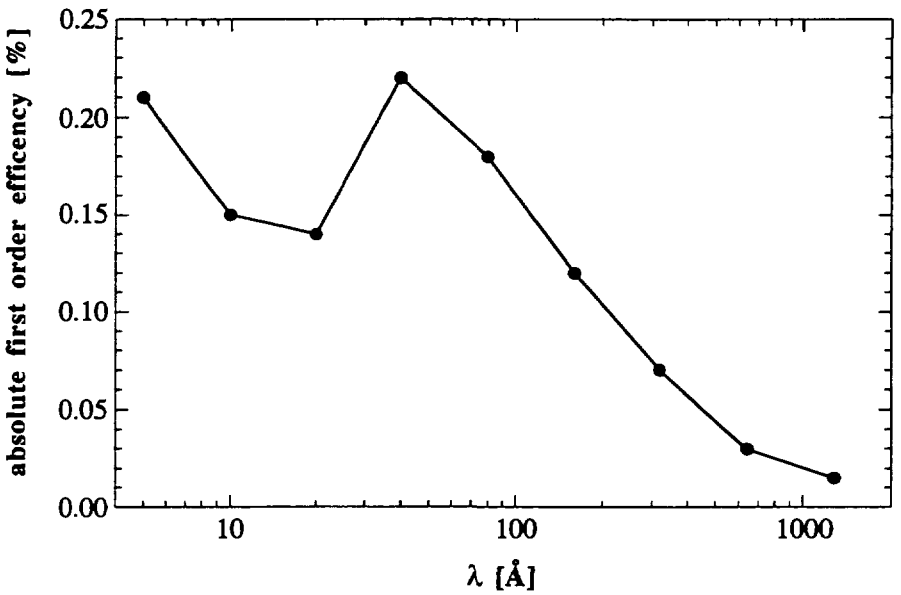

Fig. 6. Calculated overall efficiency for the VLS grating monochromator as specified in the text.

The aberrations are calculated as ray displacements in the virtual-image plane and then converted to a wavelength error using the reciprocal linear dispersion (the "Å/mm") given by

$$\left(\frac{\partial\lambda}{\partial\Delta y'}\right)_{\beta} = \frac{d\cos\beta}{mr'}. \tag{16}$$

The wavelength error due to a grating slope error δ is calculated from

$$\frac{m\Delta\lambda}{d} = \delta(\cos\alpha - \cos\beta) \tag{17}$$

and the source-size limit is found from

$$\Delta\lambda_s = \frac{sd\cos\alpha}{mr} \tag{18}$$

Resolution

The major contributions to the resolution of the simple system that we described above are represented in Fig. 7. The main point to note is that the source size of 0.1 mm (which is realistic for a third-generation synchrotron light source) is the most important limit. We do not have to accept this as being unchangeable but suppose that we decide to use the monochromator as defined so far; without an entrance slit. The resolution is still good enough for essentially all condensed matter research and, in spite of its simplicity, the system provides an impressive array of features as described in the next section.

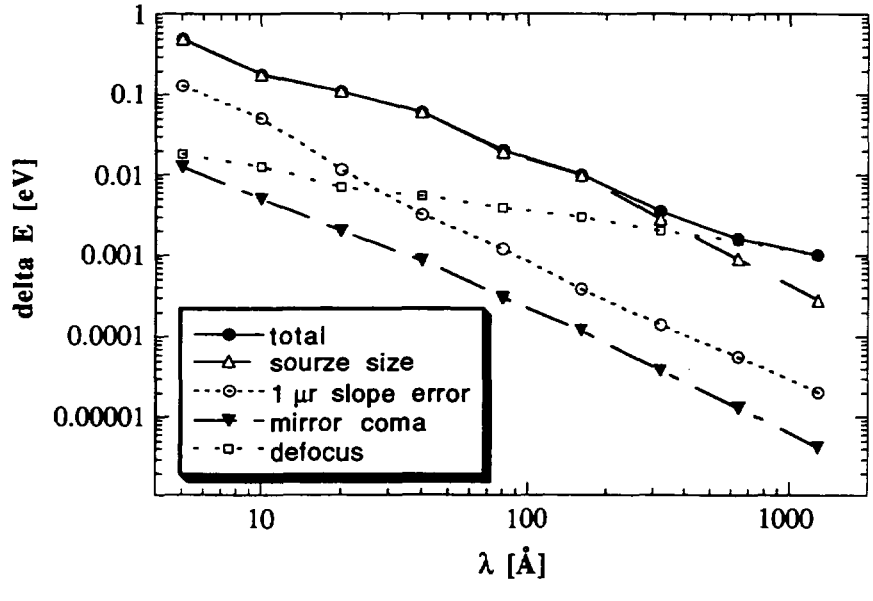

Fig. 7 Wave length dependent energy resolution calculated for the VLS grating showing the different contributions

On the other hand suppose we desire to aim for ultrahigh resolution (>20000). In this case we would certainly choose to have a real entrance slit (say of 10 μm) to replace the source which would reduce the source-size-limited bandwidth by a factor of ten. This would leave the source size, fabrication tolerances and focus error sharing in setting the limit to resolution and the resolving power would be around 20000 over most of the range. One could

push still further. We can go below 10 μm slit width and we can get better than 1 μrad optics. If we succeed with this, the limit would then come down to the focus error which, under present conditions, gives a resolving power which varies linearly from about 10^5 at 5 Å to 10^4 at 1280 Å. Broadly the slit size and optical quality dominate at the shorter wavelengths and the defocus at the longer ones. A denser grating helps with slit size and slope error but a coarser one helps with defocus. The general effect is that multiple gratings may not give a benefit in proportion their cost. The ultimate achievable resolution at the shorter wavelengths is thus determined by similar factors to other (non VLS) instruments although VLS enables the design to be simpler and more flexible. At longer, but still grazing-incidence, wavelengths the standard of comparison is the work of Schultz et al.[26] who obtained 1 meV resolution at 190 Å using an ALS SGM with moving slits. The present system (with fixed slits) would not do that but it could do 2.3 meV with a 300/mm grating or 2.9 meV with a 600/mm one. At 1000 Å the resolution drops further compared to the best attainable (which would now be with a normal-incidence system) but 1 meV is still achieved which is good for many purposes. Remember we are speaking about a single grating covering eight octaves!

General discussion

The main conclusion is that the addition of VLS to this very simple design produces a monochromator with unique properties. We may list its positive features as follows:

- Single grating
- Exceptional wavelength coverage (eight octaves)
- The system is essentially in focus at all angles. Focus errors arise only when the small-angle approximation is not satisfied. Therefore there is no need to get focus by programming the included angle which can be regarded as a user-controlled variable to optimize for order suppression or efficiency or both
- Resolution with a third-generation light source is sufficient for essentially all condensed matter research without use of an entrance slit
- Better resolution can be had by choosing or retrofitting an entrance slit
- The VLS grating can be retrofitted to any SX700 monochromator but the position or focal length of the focusing mirror may have to change
- The intrinsically large astigmatism of the SX700 configuration (or any other plane grating scheme) can be corrected by the VLS

Its main negative feature is that when the defocus error begins to play a role in determining the resolution, which is above about 50-100 Å for a 10 μm source and almost never for a 100 μm one, there is no good way to correct it. We reject moving slits or an adaptive focusing

mirror because they represent a change of philosophy while reducing the aperture provides only a partial answer with a linear price in flux. Unlike the conventional SX700 there is no included angle which corrects the focus. This is not to say that changes of the included angle do not affect the resolution in other ways. In fact increasing the included angles improves both the source-size limit and the slope error limit.

Footnote

The name primary coma has become so established that it is difficult to change. However, it is strictly incorrect and the error goes beyond pure semantics as was first pointed out by Underwood (private communication). The matter is discussed further by one of us[27].

References

1. M. C. Hettrick, S. Bowyer, "Variable line-space gratings: new design for use in grazing incidence spectrometers", *Appl. Opt.*, **22**, 3921-3924 (1983).

2. M. C. Hettrick, "Aberration of varied line-space grazing incidence gratings", *Appl. Opt.*, **23**, 3221-3235 (1984).

3. M. C. Hettrick, "Varied line-space gratings: past present and future" Proc. SPIE, vol. 560, 96, (SPIE, Bellingham, 1985).

4. M. C. Hettrick, J. H. Underwood, "Varied-Space Grazing Incidence Gratings in High Resolution Scanning Spectrometers" in *Short Wavelength Coherent Radiation: Generation and Applications* J. B. D. T. Attwood, (Ed.) vol. 147, 237-245, (American Institute of Physics Conference Proceedings, 1987).

5. J. H. Underwood, E. M. Gullikson, M. Koike, P. J. Batson, P. E. Denham, K. D. Frank, R. E. Tackaberry, W. F. Steele, "Calibration and standards beam line 6.3.2 at the Advanced Light Source", *To be published in Rev. Sci. Inst.*, , (1996).

6. T. Harada, "Design and Application of a Varied-Space Plane Grating Monochromator for Synchrotron Radiation", *Nucl. Inst. Meth.*, **A291**, 179-184 (1990).

7. T. Harada, M. Itou, T. Kita, "A Grazing-Incidence Monochromator with a Varied-space Plane Grating for Synchrotron Radiation", *Application, Theory and Fabrication of Periodic Structures*, **Proc. SPIE, 503**, 114-8 (1984).

8. T. Harada, T. Kita, "Mechanically Ruled Aberration-Corrected Concave Gratings", *Appl. Opt.*, **19**, 3987-3993 (1980).

9. M. Koike, T.Namioka, "Optimization and evaluation of varied line spacing plane grating monochromators for third generation synchrotron radiation sources" in *Vacuum Ultraviolet Radiation Physics (VUV11)* F. J. Wuilleumier, Y. Petrof, I. Nenner, (Eds.), 73-84, (World Scientific, Singapore, 1995).

10. M. Koike, T. Namioka, "High-resolution grazing incidence plane grating monochromator for undulator radiation", *Rev. Sci. Instrum.*, **66**, 2144-6 (1995).

11. M. Koike, "Beam splitting of undulator radiation with variable spacing plane grating monochromator", *Nucl. Instrum. Meth.*, **A319**, 135-140 (1992).

12. T. Namioka, M. Koike, "Analytical representation of spot diagrams and it application to the design of monochromator", *Nucl. Instrum. Meth.*, **A319**, 219-227 (1992).

13. H. Höchst, M. Bissen, M. A. Engelhardt, D. Crossley, "Design study of a high resolution soft x-ray monochromator with a movable variable density grating", *Nucl. Instrum. Meth.*, **A319**, 121-127 (1992).

14. W. R. McKinney, C. Palmer, "Design of grazing incidence monochromators involving unconventional gratings" in *Raman Scattering, Luminescence, and Spectroscopic Instrumentation in Technology*Proc. SPIE, vol. 1055, 332-335, (SPIE, Bellingham, 1989).

15. W. R. McKinney, "Varied line-space gratings and applications", *Rev. Sci. Inst.*, **63**, 1410-1414 (1992).

16. C. Palmer, W. R. McKinney, "Imaging theory of plane-symmetric varied line-spacing grating systems", *Opt. Eng.*, **33**, 820-829 (1994).

17. C. Palmer, W. R. McKinney, "Equivalence of focusing conditions for holographic and varied line space gratings", *Appl. Opt.*, **29**, 47-51 (1994).

18. T. A. Callcott, W. L. O'Brien, J. J. Jia, Q. Y. Dong, D. L. Ederer, R. N. Watts, D. R. Mueller, "A simple variable line spacing monochromator for synchrotron light source beamlines", *Nucl. Instrum. Meth.*, **A319**, 128-134 (1992).

19. H. Petersen, "The Plane Grating and Elliptical Mirror: a new Optical Configuration for Monochromators", *Opt. Comm.*, **40**, 402-6 (1982).

20. M. Hettrick, J. H. Underwood, "Optical system for high resolution spectrometer/monochromator", *United States Patent number 4776696*, , (1988).

21. H. Noda, T. Namioka, M. Seya, "Geometrical Theory of the Grating", *J. Opt. Soc. Am.*, **64**, 1031-6 (1974).

22. M. Abramowitz, I. Stegun, *Handbook of Mathematical Functions*, , (Dover, New York, 1968)

23. M. R. Howells, "Gratings and Monochromators" in *X-ray Data Booklet (PUB 490)* J. K. e. al, (Ed.) 5-25 to 5-32, (Center for X-ray Optics, Lawrence Berkeley Laboratory, Berkeley, 1986).

24. W. Welford, "Aberration Theory of Gratings and Grating Mountings" in *Progress in Optics* E. Wolf, (Ed.) vol. 4, 241-280, 1965).

25. H. Hogrefe, M. R. Howells, E. Hoyer, "Application of Spherical Gratings in Synchrotron Radiation Spectroscopy" in *Soft X-ray Optics and Technology* E.-E. Koch, G. Schmahl, (Eds.), Proc. SPIE., vol. 733, 274-285, (SPIE, Bellingham, 1986).

26. K. Schultz, G. Kaindl, M. Domke, J. D. Bozek, P. A. Heimann, A. S. Schlachter, "Observation of new Rydberg series and resonances in doubly-excited helium at ultra-high resolution", *Submitted to Phys. Rev. Lett.*, , (1996).

27. M. R. Howells, "Mirrors for Synchrotron Radiation Beam Lines" in *New Directions in Research with Third-Generation Soft X-ray Sources* A. S. Schlachter, F. J. Wuilleumier, (Eds.), , (Kluwer, London, 1994).

Appendix 1: Incident and reflected angels, focal length, aberration due to defocus, aberration due to coma (with v1 and * v1 and v2 corrected), and overall efficiency for the VLS grating upon different x-ray energies/wave lengths.

λ [Å]	E [eV]	α°	β°	Focal length [m]	Δ_{defoc} [μm]	Δ_{coma} [μm]	Δ^*_{coma} [μm]	$\Delta y'_{lc}$ [μm]	efficency
0	-	89	-89	-15	0	0	0	0	
5	2480	89.5	-88.51	-14.998	0.62	15.8	0.009	0.086	0.21
10	1240	89.3	-87.90	-14.995	1.25	11.4	0.013	0.122	0.15
20	620	88	-86.55	-14.988	1.73	1.71	0.006	0.150	0.14
40	310	86	-84.36	-14.973	3.18	0.53	0.006	0.183	0.22
80	165	85	-82.48	-14.948	6.56	0.51	0.009	0.274	0.18
160	77.5	80	-77.22	-14.883	12.5	0.16	0.009	0.323	0.12
320	38.7	78	-73.53	-14.778	25.6	0.18	0.016	0.500	0.07
640	19.4	75	-68.05	-14.573	53	0.19	0.026	0.748	0.03
1280	9.7	70	-59.64	-14.160	110	0.18	0.043	1.076	0.02